

DOI: 10.1002/anie.200501349

**Observation of Weak C–H...O Hydrogen Bonding to Unactivated Alkanes\*\****Xue-Bin Wang, Hin-Koon Woo, Boggavarapu Kiran, and Lai-Sheng Wang\**

The hydrogen bond plays an essential role in chemistry and biochemistry.<sup>[1]</sup> It generally has the form X–H...Y, where X and Y are highly electronegative atoms such as O or N. The fact that a relatively less electronegative carbon can also behave as a proton donor to form C–H...O-type hydrogen bonds has been the subject of controversy for many years.<sup>[2–4]</sup> However, it is now well accepted and has been identified in many biological systems<sup>[5–13]</sup> and crystal engineering.<sup>[14–18]</sup> Most C–H...O hydrogen bonds have been observed for the so-called activated C, where the hydrogen-donor C atom is attached to electronegative groups such as halogen atoms or NH groups in the protein backbone. In biological systems or molecular crystals, C–H...O hydrogen bonds are usually accompanied by other stronger molecular interactions that make it difficult to evaluate their relative contributions. Despite the importance of the C–H...O hydrogen bond and extensive theoretical studies,<sup>[19–25]</sup> its nature is still being debated,<sup>[26–29]</sup> and there have been no experimental characterizations of its strength to date. We report here the first direct experimental observation of conformation changes induced solely by C–H...O hydrogen bonding in a series of unactivated aliphatic carboxylate molecules, CH<sub>3</sub>(CH<sub>2</sub>)<sub>n</sub>CO<sub>2</sub><sup>–</sup>, in the gas phase, where the C–H...O hydrogen bonding is the only molecular interaction driving the conformational changes.

Photoelectron spectra of CH<sub>3</sub>(CH<sub>2</sub>)<sub>n</sub>CO<sub>2</sub><sup>–</sup> (*n* = 0–8) were measured at both room and low temperatures, as shown in Figure 1. We observed very similar spectra at room temperature for all the species, which all have adiabatic detachment energies (ADEs) of around 3.4 eV because the aliphatic chain

[\*] Dr. X.-B. Wang, Dr. H.-K. Woo, Dr. B. Kiran, Prof. Dr. L.-S. Wang  
Department of Physics, Washington State University  
2710 University Drive, Richland, WA 99352 (USA)  
and  
W. R. Wiley Environmental Molecular Sciences Laboratory and  
Chemical Sciences Division  
Pacific Northwest National Laboratory  
MS 8-88, P.O. Box 999, Richland, WA 99352 (USA)  
Fax: (+1) 509-376-6066  
E-mail: ls.wang@pnl.gov

[\*\*] We thank Dr. S. E. Barlow for valuable discussions. This work was supported by the U.S. Department of Energy (DOE), Office of Basic Energy Sciences, Chemical Science Division. The experiment and calculations were performed at the W. R. Wiley Environmental Molecular Sciences Laboratory, a national scientific user facility sponsored by the DOE Office of Biological and Environmental Research and located at Pacific Northwest National Laboratory, which is operated for the DOE by Battelle.

 Supporting information for this article is available on the WWW under <http://www.angewandte.org> or from the author.

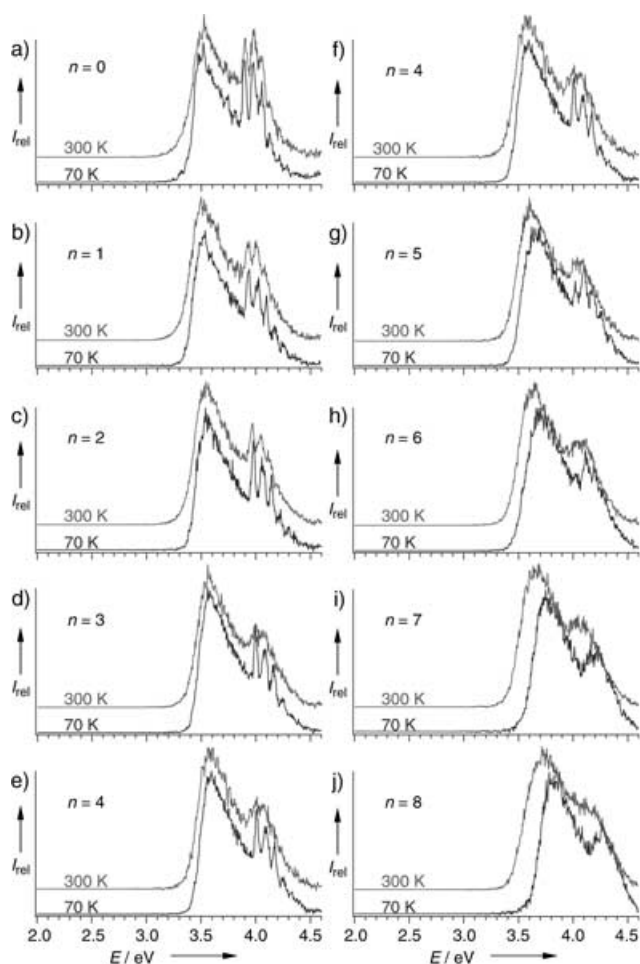


**Figure 1.** Photoelectron spectra of  $\text{CH}_3(\text{CH}_2)_n\text{CO}_2^-$  ( $n=0-8$ ) measured at 266 nm (4.661 eV) and at two different ion-trap temperatures. Note the blue shift of the 70 K spectra starting from  $n=5$ .

has very little effect on the electron binding energies of the carboxylate group. The two observed bands in all the spectra are due to detachment from three oxygen lone-pair orbitals on the carboxylate, and the first broad band actually contains two detachment channels.<sup>[30,31]</sup> The second spectral band was vibrationally resolved for  $n=0-2$ , with a vibrational frequency of about  $640\text{ cm}^{-1}$  that is characteristic of the  $\text{CO}_2$  bending motion.<sup>[32]</sup> The vibrational structure is smeared out in the larger systems in the room temperature spectra. Significant changes were observed in the PES spectra at a trapping temperature of 70 K. For  $n=0-4$  (Figure 1, left column), the low-temperature spectra are much sharper and the  $\text{CO}_2$  bending vibrational progression in the second band is much better resolved in all the spectra. The reduction of the vibrational hot band can clearly be observed by comparing the threshold regions of the spectra taken at 70 and at 300 K. For  $n=5-8$ , in addition to the spectral sharpening, the 70 K spectra surprisingly exhibit a systematic blue shift, which ranges from 50 meV for  $n=5$  to 150 meV for  $n=8$ . Vibrational structures in the second band were also resolved for these larger species, more clearly for  $n=5$  and 6, but the Franck–Condon envelope is quite different in the larger systems than in the smaller species.

The blue shift observed for  $n=5-8$  in the low-temperature spectra suggests a conformational change in which the negative charge on the carboxylate is stabilized, most likely resulting from the formation of  $\text{C-H}\cdots\text{O}$  hydrogen bonds between the terminal  $\text{CH}_3$  group and the  $-\text{CO}_2^-$  group to form a folded structure.<sup>[32,33]</sup> Because of the anticipated weakness of this  $\text{C-H}\cdots\text{O}$  hydrogen bonding, the folded conformation can only be observed at lower temperatures owing to the large entropy contributions at higher temperatures for the linear structure. To obtain further insight into the folding transition, we performed temperature-dependent studies for  $n=6$  and 8 at trapping temperatures from 300 to 18 K (Figure 2). For

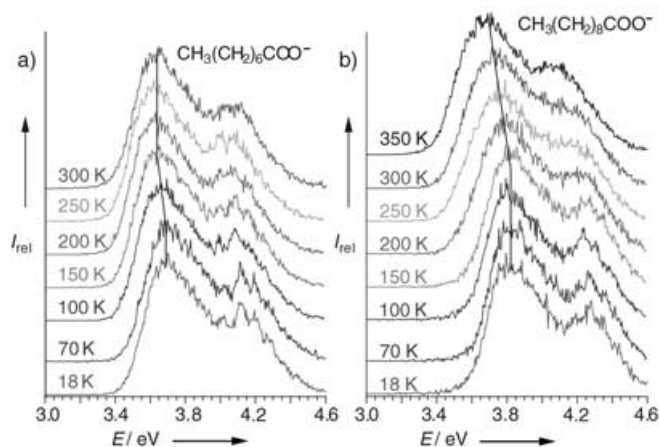


**Figure 2.** Temperature-dependent photoelectron spectra of  $\text{CH}_3(\text{CH}_2)_6\text{CO}_2^-$  and  $\text{CH}_3(\text{CH}_2)_8\text{CO}_2^-$ . The lines drawn are intended to guide the eyes and have no other significance.

$\text{CH}_3(\text{CH}_2)_6\text{CO}_2^-$  there was no observable blue shift from 300 K to 200 K, but at 150, 100, and 70 K the PES spectra exhibit successive blue shifts of about 10, 10, and 40 meV, respectively. The spectrum shows no blue shift upon further cooling the trap to 18 K. These observations suggest that the folding transition starts at around 150 K for  $\text{CH}_3(\text{CH}_2)_6\text{CO}_2^-$ , and at around 70 K all the anions are already in the folded conformation due to the  $\text{C-H}\cdots\text{O}$  hydrogen bonding. For  $\text{CH}_3(\text{CH}_2)_8\text{CO}_2^-$ , a blue shift of about 30 meV was already observed upon cooling the trap from 300 K to 250 K. Further blue shifts of about 45 and 65 meV were observed at 200 and 150 K, respectively. No measurable shift was observed upon further cooling, which suggests that at 150 K all the  $\text{CH}_3(\text{CH}_2)_8\text{CO}_2^-$  anions are already in the folded conformation. The blue shift observed immediately upon cooling from 300 K indicates that there might already be folded conformations present at room temperature for  $\text{CH}_3(\text{CH}_2)_8\text{CO}_2^-$ . We therefore made one more measurement by heating the ion trap to 350 K, and indeed observed a red shift relative to the 300 K spectrum by about 50 meV. The 300 K spectrum seems to be slightly broader than the 350 K spectrum, which is consistent with the fact that both linear and folded conformations coexist at room temperature. The ADE of  $\text{CH}_3(\text{CH}_2)_8\text{CO}_2^-$  at 350 K is now about 3.47 eV, similar to those of the smaller species, thus indicating that the linear structure dominates for  $\text{CH}_3(\text{CH}_2)_8\text{CO}_2^-$  only at 350 K.

Our temperature-dependent PES data yielded the following blue shifts between the folded and linear structures: 50, 60, 130, and 190 meV for  $n=5-8$ , respectively. These shifts reflect the stabilization of the negative charge on the  $-\text{CO}_2^-$  group by the  $\text{C}-\text{H}\cdots\text{O}$  hydrogen bonding, as illustrated in Figure 3. As the strength of the  $\text{C}-\text{H}\cdots\text{O}$  hydrogen bonding in

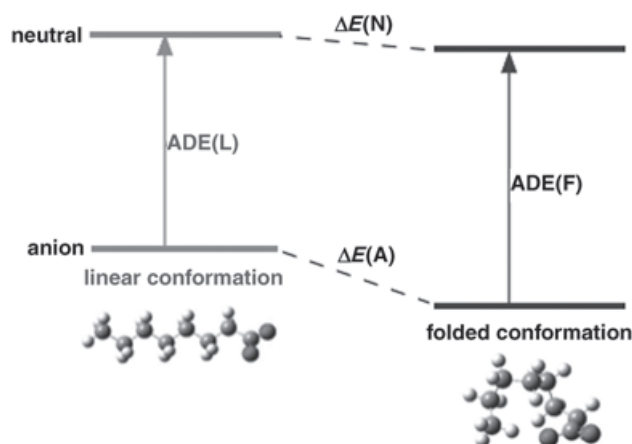


**Figure 3.** The energetic relationships between the anions and the neutral species and between the linear and folded configurations. ADE(L) and ADE(F) are the adiabatic detachment energies of the linear and folded conformations, respectively.  $\Delta E(A)$  and  $\Delta E(N)$  are the stabilization energies of the folded relative to the linear conformations for the anions and neutrals, respectively. The stabilization energies have two components, the  $\text{C}-\text{H}\cdots\text{O}$  hydrogen-bonding energies in the folded conformations ( $E_H(A)$  and  $E_H(N)$  for the anions and neutrals, respectively) and the strain energies in the folded backbones ( $E_S(A)$  and  $E_S(N)$  for the anions and neutrals, respectively). The strain energies in the anions and neutrals are expected to be similar for a given chain length. Thus, the measured spectral shift ( $\Delta\text{ADE}$ ) between the folded and linear conformations is equivalent to the difference of the  $\text{C}-\text{H}\cdots\text{O}$  hydrogen-bond strength in the anions and neutrals:  $\Delta\text{ADE} = -\text{ADE}(F) - \text{ADE}(L) = \Delta E(A) - \Delta E(N) = E_H(A) - E_H(N)$ .

the neutral  $\text{CH}_3(\text{CH}_2)_n\text{CO}_2\cdot$  radical is expected to be small ( $0.5 \text{ kcal mol}^{-1}$  or less),<sup>[20]</sup> the observed blue shifts provide lower limits for the  $\text{C}-\text{H}\cdots\text{O}$  hydrogen bonding strength in the  $\text{CH}_3(\text{CH}_2)_n\text{CO}_2^-$  anions (1.2, 1.4, 3.0, and  $4.4 \text{ kcal mol}^{-1}$  for  $n=5-8$ , respectively).

To obtain further insight into the nature of the  $\text{C}-\text{H}\cdots\text{O}$  hydrogen bonding in the  $\text{CH}_3(\text{CH}_2)_n\text{CO}_2^-$  anions, we performed theoretical calculations on the linear and folded conformations for  $n=3-8$  (Figure 4). We found that the folded conformations are more stable than the linear structures in all cases. However, we also observed that there is no  $\text{C}-\text{H}\cdots\text{O}$  hydrogen-bonding interaction in the cases of  $n=3$  and 4 because either the  $\text{CH}\cdots\text{O}$  distances or the  $\angle\text{C}-\text{H}\cdots\text{O}$  angles are outside the normal ranges expected for such interactions. One  $\text{C}-\text{H}\cdots\text{O}$  hydrogen bond was observed for  $n=5$  and 6, whereas for  $n=7$  and 8 two  $\text{C}-\text{H}\cdots\text{O}$  hydrogen bonds are formed, consistent with the large ADE shifts observed for these two species in the PES spectra at low temperature. The calculations also revealed that the two  $\text{C}-\text{O}$  bond lengths become different upon hydrogen-bond formation as a result of the charge localization onto the hydrogen-bonded O atom. The abrupt change in the  $\text{CO}_2$  bending

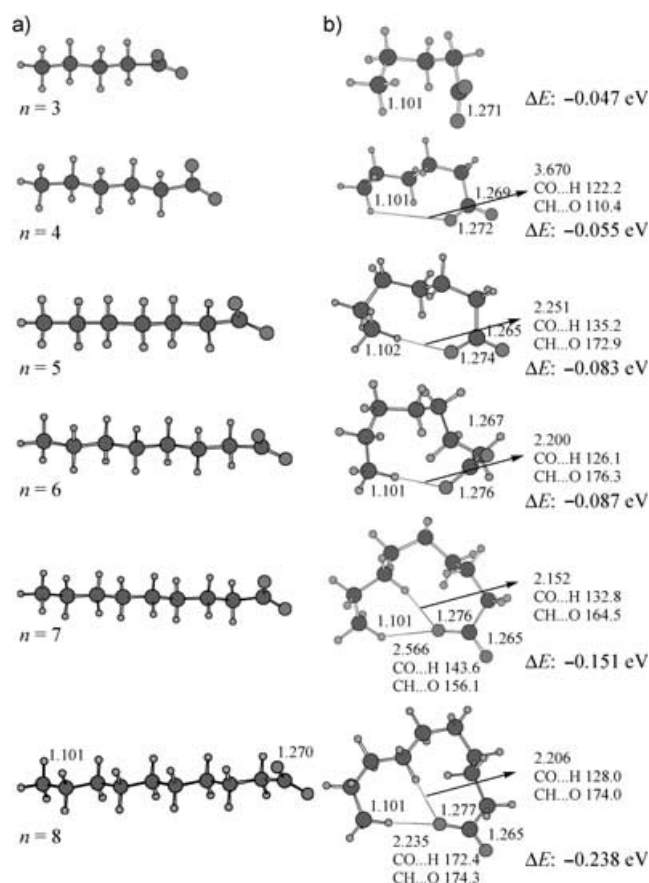


**Figure 4.** Optimized structures for the a) linear and b) folded conformations of  $\text{CH}_3(\text{CH}_2)_n\text{CO}_2^-$  ( $n=3-8$ ) at the MP2/aug-cc-pVDZ level of theory. Selected  $\text{C}-\text{H}$ ,  $\text{C}-\text{O}$ , and  $\text{H}\cdots\text{O}$  bond distances are indicated in Å. The  $\text{CO}\cdots\text{H}$  and  $\text{CH}\cdots\text{O}$  bond angles are given in degrees.  $\Delta E$ : the stabilization energies of the folded relative to the linear conformation.

vibrational progression in the second PES band for  $n=5-8$  is consistent with the subtle geometric changes as a result of the  $\text{C}-\text{H}\cdots\text{O}$  hydrogen-bond formation. The  $\text{C}-\text{H}\cdots\text{O}$  hydrogen-bond strengths are different in each system owing to the different steric effects that lead to different  $\text{C}-\text{H}\cdots\text{O}$  hydrogen-bonding geometries. The strengths of the two  $\text{C}-\text{H}\cdots\text{O}$  hydrogen bonds in the  $n=7$  and 8 species are also not equivalent. However, an average bond strength for each  $\text{C}-\text{H}\cdots\text{O}$  hydrogen bond in  $n=7$  and 8 can be obtained from the PES spectral shifts. Thus, we obtained the following lower limits of the bond strength for a single  $\text{C}-\text{H}\cdots\text{O}$  hydrogen bond in  $\text{CH}_3(\text{CH}_2)_n\text{CO}_2^-$ : 1.2, 1.4, 1.5, and  $2.2 \text{ kcal mol}^{-1}$  for  $n=5-8$ , respectively.

Unactivated alkanes form the weakest  $\text{C}-\text{H}\cdots\text{O}$  hydrogen bonds.<sup>[20]</sup> For example, the calculated  $\text{C}-\text{H}\cdots\text{O}$  hydrogen-bond strength in the  $\text{H}_2\text{C}=\text{O}/\text{CH}_4$  complex is only  $0.46 \text{ kcal mol}^{-1}$  which increases to  $1.2 \text{ kcal mol}^{-1}$  in  $\text{H}_2\text{C}=\text{O}/\text{CH}_3\text{F}$ .<sup>[20]</sup> The relatively large  $\text{C}-\text{H}\cdots\text{O}$  hydrogen-bond strength in  $\text{CH}_3(\text{CH}_2)_n\text{CO}_2^-$  is due to the negative charge on the carboxylate group, which usually forms a strong ionic hydrogen bond.<sup>[34]</sup> Thus, even unactivated alkanes can form relatively strong  $\text{C}-\text{H}\cdots\text{O}$  hydrogen bonds to strong acceptors. The current work provides the first examples that pure  $\text{C}-$

H...O hydrogen bonding can play a significant structural role in determining molecular conformations. These results should have major implications to assess the role of C-H...O hydrogen bonding in biological structures and reactivities. The quantitative experimental data can also be used to verify theoretical calculations and help evaluate the dependence of the C-H...O hydrogen-bond strength on its geometry. We have also demonstrated that the low-temperature capability is not only valuable to remove vibrational hot bands and enhance photoelectron spectral resolution, but also opens up new research opportunities and allows weak molecular interactions to be isolated and investigated.

### Experimental Section

Low-temperature photoelectron spectroscopy with electrospray: The experiments were carried out with a brand new home-built instrument that couples electrospray ionization with a magnetic-bottle time-of-flight photoelectron spectrometer, with a new capability of being able to control the ion temperatures. The electrospray source and the magnetic-bottle photoelectron spectrometer are similar to those described previously.<sup>[35]</sup> Briefly, the anions of interest,  $\text{CH}_3(\text{CH}_2)_n\text{CO}_2^-$  ( $n=0-8$ ), were produced from solutions of the corresponding acids under slightly basic conditions in a mixed methanol/water solvent (3/1 volume ratio). Anions from the source were guided by a RF-only octopole device into a quadrupole mass filter, which was operated in the RF-only mode in the current experiment. Following the mass filter, the ion beam was guided by a 90 degree ion bender into a 3D Paul trap, which was attached to the cold head of a closed-cycle helium refrigerator. The temperature of the cold head can be controlled between 10–350 K. A portion of the incoming ions was trapped and collisionally cooled with a background gas ( $\approx 1$  mTorr  $\text{N}_2$  in most cases for temperatures between 350–70 K, or 5%  $\text{H}_2$  in helium for lower-temperature operations). The ions were trapped for a period of 20–100 ms and cooled by translational and rovibrational energy transfers to the background gas (the number of collisions was estimated to be about 2000–10000). The trap was operated at low  $q$  values ( $< 0.3$ ) to avoid RF heating.<sup>[36,37]</sup> The trapped ions were pulsed out into the extraction zone of a time-of-flight mass spectrometer at a 10 Hz repetition rate.

The ions of interest were mass-selected and decelerated before being intercepted with a 266-nm laser beam in the interaction zone of the magnetic-bottle photoelectron analyzer. The laser was operated at a 20 Hz repetition rate with the ion beam off at alternate shots for background subtraction. The photodetached electrons were collected with nearly 100% efficiency by the magnetic-bottle and analyzed in a 5-meter-long electron flight tube. The electron energy resolution was  $\Delta E/E \approx 2\%$ , i.e., 20 meV for 1 eV electrons. Photoelectron time-of-flight spectra were collected and then converted into kinetic energy spectra, calibrated by the known spectra of  $\text{ClO}_2^-$ <sup>[33]</sup> and  $\text{I}^-$ . The electron binding energy spectra presented were obtained by subtracting the kinetic energy spectra from the detachment photon energies.

Two known anions,<sup>[38,39]</sup>  $\text{ClO}_2^-$  and  $\text{C}_{60}^-$ , were used to test the effectiveness of the ion cooling. At a trap temperature of 70 K, vibrational hot bands in the photoelectron spectrum of  $\text{ClO}_2^-$  were completely removed. At the same trap temperature, vibrational hot bands were still detectable in the photoelectron spectrum of the relatively large  $\text{C}_{60}^-$  anion, whose vibrational temperature was estimated to be about 100 K, which yields a difference of around 30 K between the trapping temperature and the  $\text{C}_{60}^-$  vibrational temperature. We expected that this difference would be smaller for the  $\text{CH}_3(\text{CH}_2)_n\text{CO}_2^-$  anions because of their relatively smaller size.

Theoretical methods: All calculations were performed with the programs Gaussian 03<sup>[40]</sup> and NWChem.<sup>[41]</sup> An initial search of the

stable conformers was done with local density functional theory (LSDA) with an augmented correlation consistent polarized valence double- $\zeta$  basis set (aug-cc-pVDZ). The lowest energy geometries were used for geometry optimization at the second-order Moller-Plesset Perturbation Theory (MP2) level with the same basis set. Frequencies and other thermodynamic values were calculated at the LSDA level. All DFT calculations were performed with Gaussian 03 and MP2 optimizations with NWChem.

Received: April 19, 2005

Published online: July 8, 2005

**Keywords:** alkanes · conformation analysis · density functional calculations · hydrogen bonds · photoelectron spectroscopy

- [1] G. A. Jeffrey, W. Saenger, in *Hydrogen Bonding in Biological Structures*, Springer, Berlin, **1991**.
- [2] D. J. Sutor, *Nature* **1962**, *195*, 68–69.
- [3] R. Taylor, O. Kennard, *J. Am. Chem. Soc.* **1982**, *104*, 5063–5070.
- [4] G. R. Desiraju, *Acc. Chem. Res.* **1991**, *24*, 290–296.
- [5] T. Steiner, W. Saenger, *J. Am. Chem. Soc.* **1992**, *114*, 10146–10154.
- [6] Z. S. Derewenda, L. Lee, U. Derewenda, *J. Mol. Biol.* **1995**, *252*, 248–262.
- [7] J. Bella, H. M. Berman, *J. Mol. Biol.* **1996**, *264*, 734–742.
- [8] M. C. Wahl, S. T. Rao, M. Sundaralingam, *Nat. Struct. Biol.* **1996**, *3*, 24–31.
- [9] I. Berger, M. Egli, A. Rich, *Proc. Natl. Acad. Sci. USA* **1996**, *93*, 12116–12121.
- [10] M. C. Wahl, M. Sundaralingam, *Trends Biochem. Sci.* **1997**, *22*, 97–101.
- [11] E. L. Ash, J. L. Sudmeier, R. M. Day, M. Vincent, E. V. Torchilin, K. C. Haddad, E. M. Bradshaw, D. G. Sanford, W. W. Bachovchin, *Proc. Natl. Acad. Sci. USA* **2000**, *97*, 10371–10376.
- [12] K. M. Lee, H.-C. Chang, J.-C. Jiang, J. C. C. Chen, H.-E. Kao, S. H. Lin, I. J. B. Lin, *J. Am. Chem. Soc.* **2003**, *125*, 12358–12364.
- [13] M. Motamal, T. Lazaridis, *Biochemistry* **2005**, *44*, 1607–1613.
- [14] G. R. Desiraju, *Acc. Chem. Res.* **1996**, *29*, 441–449.
- [15] K. N. Houk, S. Menger, S. P. Newton, F. M. Raymo, J. F. Stoddart, D. J. Williams, *J. Am. Chem. Soc.* **1999**, *121*, 1479–1487.
- [16] E. May, R. Destro, C. Gatti, *J. Am. Chem. Soc.* **2001**, *123*, 12248–12254.
- [17] C. K. Broder, M. G. Davidson, V. T. Forsyth, J. A. K. Howard, S. Lamb, S. A. Mason, *Cryst. Growth Des.* **2002**, *2*, 163–169.
- [18] J. A. van der Berg, K. R. Seddon, *Cryst. Growth Des.* **2003**, *3*, 643–661.
- [19] Y. Gu, T. Kar, S. Scheiner, *J. Am. Chem. Soc.* **1999**, *121*, 9411–9422.
- [20] R. Vargas, J. Garza, D. A. Dixon, B. P. Hay, *J. Am. Chem. Soc.* **2000**, *122*, 4750–4755.
- [21] M. Hartmann, S. D. Wetmore, L. Radom, *J. Phys. Chem. A* **2001**, *105*, 4470–4479.
- [22] S. Scheiner, S. J. Grabowski, T. Kar, *J. Phys. Chem. A* **2001**, *105*, 10607–10612.
- [23] Y. Tatamitani, B. Liu, J. Shimada, T. Ogata, P. Ottaviani, A. Maris, W. Caminati, J. S. Alanso, *J. Am. Chem. Soc.* **2002**, *124*, 2739–2743.
- [24] A. Kovacs, A. Szabo, D. Nemcsok, S. Hargittai, *J. Phys. Chem. A* **2002**, *106*, 5671–5678.
- [25] H. B. Guo, R. F. Beahm, H. Guo, *J. Phys. Chem. B* **2004**, *108*, 18065–18072.
- [26] P. Hobza, Z. Havlas, *Chem. Rev.* **2000**, *100*, 4253–4264.
- [27] S. Scheiner, T. Kar, *J. Phys. Chem. A* **2002**, *106*, 1784–1789.
- [28] X. Li, L. Liu, H. B. Schlegel, *J. Am. Chem. Soc.* **2002**, *124*, 9639–9647.

- [29] W. Qian, S. Krimm, *J. Phys. Chem. A* **2002**, *106*, 6628–6636.
- [30] E. H. Kim, S. E. Bradforth, D. W. Arnold, R. B. Metz, D. M. Neumark, *J. Chem. Phys.* **1995**, *103*, 7801–7814.
- [31] Z. Lu, R. E. Continetti, *J. Phys. Chem. A* **2004**, *108*, 9962–9969.
- [32] K. Norrman, T. B. McMahon, *J. Phys. Chem. A* **1999**, *103*, 7008–7016.
- [33] J. Catalan, *Chem. Phys. Lett.* **1994**, *221*, 68–70.
- [34] M. Meot-Ner, *Chem. Rev.* **2005**, *105*, 213–284.
- [35] L. S. Wang, C. F. Ding, X. B. Wang, S. E. Barlow, *Rev. Sci. Instrum.* **1999**, *70*, 1957–1966.
- [36] J. F. J. Todd, *Mass Spectrom. Rev.* **1991**, *10*, 3–52.
- [37] E. R. Lovejoy, R. Bianco, *J. Phys. Chem. A* **2000**, *104*, 10280–10287.
- [38] M. K. Gilles, M. L. Polak, W. C. Lineberger, *J. Chem. Phys.* **1992**, *96*, 8012–8020.
- [39] X. B. Wang, C. F. Ding, L. S. Wang, *J. Chem. Phys.* **1999**, *110*, 8217–8220.
- [40] Gaussian 03 (Revision B.04): M. J. Frisch et al., see Supporting Information.
- [41] High Performance Computational Chemistry Group NWChem (Version 4.5), A Computational Chemistry Package for Parallel Computers, Pacific Northwest National Laboratory, Richland, WA, **2002**.